Gradients and Active Contour Models for Localization of Cell Membrane in HER2/neu Images

Marek Wdowiak[1(✉)], Tomasz Markiewicz[1,2], Stanislaw Osowski[1,3], Janusz Patera[2], and Wojciech Kozlowski[2]

[1] Warsaw University of Technology, 1 Politechniki Sq., 00-661 Warsaw, Poland
{wdowiakm,markiewt,sto}@iem.pw.edu.pl
[2] Military Institute of Medicine, 128 Szaserow Str., 04-141 Warsaw, Poland
{jpatera,wkozlowski}@wim.mil.pl
[3] Military University of Technology,
2 Gen. S. Kaliskiego Str., 00-908 Warsaw, Poland

Abstract. The paper presents an application of the snake model to recognition of the cell membrane in the HER2 breast and kidney cancer images. It applies the modified snake to build the system recognizing the membrane and associating it with the neighboring cell. We study different forms of gradient estimation, the core point in the snake model. The particle swarm optimization algorithm is used in tuning the parameters of the snake model. On the basis of the applied procedure the estimation of the membrane continuity of cell is made. The experimental results performed on 100 cells in breast and 100 cells in kidney cancers have shown high accuracy of the membrane localizations and acceptable agreement with the expert estimations.

Keywords: Image segmentation · Object recognition · HER2/neu · Snake

1 Introduction

Recognition of the whole cells on the basis of the staining localized in the membrane is a complex task, which requires not only segmentation of the specified parts of cell, but also assigning them to the individual cells. An example of such task is in image analysis of the breast cancer created using histopathology Human Epidermal Growth Factor Receptor 2 (HER2/neu). The histopathological evaluation of a set of immunohistochemical stains is the most common task for pathologists.

The HER2/neu biomarker is recognized as a diagnostic, prognostic and predictive factor mainly in the case of breast cancer [9], but recently also discussed in kidney cancer [6]. It is indicated as an aid in assessment of breast cancer for patients for whom trastuzumab treatment is being considered. Overexpressions

G. Azzopardi and N. Petkov (Eds.): CAIP 2015, Part I, LNCS 9256, pp. 432–444, 2015.
DOI: 10.1007/978-3-319-23192-1_36

of HER2 protein connected with the HER2 gene amplification are diagnosed in approximately 20% of the analyzed breast cancer cases. For such patients, the trastuzumab treatment is recommended. Otherwise, HER2 is frequently expressed in normal renal tissues but rarely expressed in renal cell carcinoma (RCC) tissues [6]. Furthermore, the HER2 status of normal tissue is negatively correlated with that of the RCC tissues and the TNM stages, suggesting that HER2 is involved in RCC oncogenesis. Thus, an appropriate and reliable evaluation of HER2 status is necessary.

The HER2/neu stain is regarded as a basic step in pathomorphological evaluation of the breast cancer. This semiquantitative examination, performed on the immunestained paraffin section needs determining the presence, intensity, and continuity of membrane staining in the tumor cells. Four categories in grade scale are recognized: 0 (no membrane staining is observed or membrane staining is observed in less than 10% of the tumor cells), 1+ (a barely perceptible membrane staining is detected in more than 10% of tumor cells, the cells exhibit incomplete membrane staining), 2+ (a weak to moderate complete membrane staining observed in more than 10% of tumor cells), and 3+ (a strong complete membrane staining observed in more than 10% of tumor cells). The case 0 or 1+ indicates no HER2 gene amplification. On the other side grade 3+ indicates immediate HER2 gene amplification. The case 2+ needs additional examination using the fluorescence in situ hybridization (FISH) [9]. However, in kidney cancer there are still not clear guidelines as to how to assess HER2 status. Nevertheless, the main aspect of presented methodology is localizing and assigning the immunoreactive membrane to the individual cell. Whereas a lot of algorithms for the nuclear reactions have been developed [3,7,8], the HER2/neu membrane reaction is still treated manually or in a very rough way, not taking into account the separate cells.

In the last years some new approaches to solve this problem have been proposed. To such methods belong the application of the realtime quantitative polymerase chain reaction (PCR) using LightCycler [10], application of support vector machine [4], or fuzzy decision tree by using Mamdani and Takagi-Sugeno inference rules [13]. In spite of existing methods the new approaches are needed, because of the problems with high variability of a membrane reaction and its frequent overlapping with a cytoplasm. Such methods should deal with these difficult image analysis tasks in a more efficient way, providing higher agreement with an expert assessment.

In this paper we propose solving the problem of recognizing and assigning the membrane to the particular cell on the basis of the active contour models, called snakes, using different gradient estimations as the input attributes. We investigate the locally adaptive gradient, depending on a special relation between the cell nucleus and membrane. Our propositions are checked in the numerical experiments concerning two studied cases: the breast cancer and kidney cancer.

2 Problem Statement

An automatic evaluation of the HER2/neu membrane staining aims at the recognition of tumor cell nuclei and area of positive membrane reaction. It should specify which parts of the recognized membrane come from the specific cells and finally graduate the reaction from 0 to 3+ scale. Each of these steps requires different algorithms based on various criteria. The cell nuclei detection can be performed as a task of segmentation of the blue, rounded and generally non-touching objects. The solution of this problem was proposed by us in [15].

The main problem is a weak staining of the nuclei by the blue hematoxyline. The additional problem is their partial overlapping with the brown chromogenic substrate. The important task in this evaluation is recognition of areas with a positive membrane reaction, especially when the brown chromogenic substrate is located not only in the cell membranes, but also partially in the cell cytoplasm. In such case there is an identification problem of the appropriate membrane sections located inside the brown marked regions. Although this problem was solved by us in [15] using the hourglass shape structuring element combined with watershed algorithm there is still the problem of association of the discovered membrane segments with the proper cell, especially when the segment is touching few cells. In this paper we will solve this problem by applying the snake model of membrane [16]. On the basis of the snake results we are able to assign the membrane to the proper cell and then parametrize the localized membrane. The most important is the estimation of the continuity of the cell membrane. The continuity is defined here as the ratio of the summed lengths of membrane segments to the total length of membrane defined by the snake model.

A set of typical HER2/neu images with various grades of HER2 status are presented in Fig 1. As we can see the membrane reaction can vary from lower or higher intensity located only in a separated cell (a thin line) to a very high

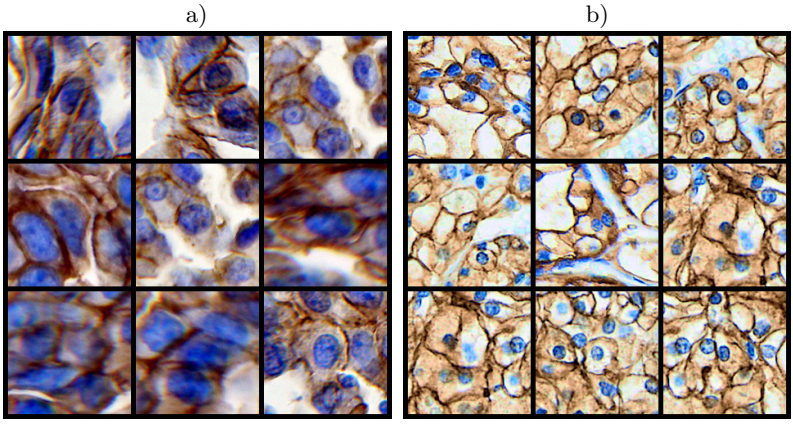

Fig. 1. The exemplary collection of cell images of breast cancer (a) and kidney cancer (b) with differences in membrane stain continuity.

intensity of the membrane location surrounded by the slightly colored cytoplasm of few touching cells. The aim of the presented study is to design method that will be able to identify any membrane positive reaction, irrespective of their intensity, different localization and character of the brown chromogenic substrate.

3 Material and Methods

The materials used in experiments come from the archive of the Pathomorphology Department in the Military Institute of Medicine in Warsaw, Poland. 125 cells of the breast and kidney cancers represented by HER2/neu preparations without any artefacts representing 1+, 2+, and 3+ grades were selected. In the case of breast cancer the analyzed data were represented by 27 cells of grade 1+, 46 cells of 2+ and 52 grades of grade 3+. The kidney cancer data were represented by 26 cells of grade 1+, 45 cells of 2+ and 54 grades of grade 3+. The paraffin embedded tissues were stained in a standard way according to the Ventana PATHWAY anti-HER-2/neu (4B5) Rabbit Monoclonal Primary Antibody protocol [1]. The specimen images were registered on the Olympus BX-61 microscope with the DP-72 colour camera under the magnification 400x and resolution 1024x768 pixels. Cells was divided in to sets: testing set with 100 cells and learning sets with 25 cells.

The quantitative analysis of the specimen needs the following steps of image processing: a) recognition of the tumor cell nuclei, b) segmentation of the immunereactive cell membranes, c) the assignment of the membrane segments to the individual cell. While the first two steps can be implemented using the set of advanced mathematical morphology transformations [11,12], the last one is very complicated due to frequent discontinuities in the membrane reaction, high variability of the cell shapes and different localizations of the cell nuclei. The classical watershed method for the individual cell separation is insufficient, as we demonstrate later.

To solve the problem, we propose to apply the snake active contour method, starting from each nucleus outline. We proceed from the nucleus to the cell contour, which is recognized on the basis of the immunoreactive membrane segments. To implement this procedure we have to select or create the most useful input image map on the basis of which we can build the gradient image, and select the most adequate parameters in the snake adaptation process. The recognized snake will represent the membrane associated with the particular cell. In the next parts of this section we introduce and compare two types of input image maps, four types of gradient and Particle Swarm Optimization method [5] for an efficient snakes parameters selection.

3.1 Input Image Map

The input map representation of the original image is crucial for a convergence of any method to an expected solution. Such map should contain the most important information about direction and distance of any pixel in the area under

interest to the cell membrane. Common approach includes the selection of color components, which allow to differentiate such area in the best way. The image map formed on the basis of these colors is subject to further analysis.

We have taken into account the following color representations: RGB, CMYK, HSV, YCbCr, CIE Lab, CIE Lch, CIE uvL, CIE XYZ [2]. The ability of different pixel intensity representations to recognize the cell membranes was evaluated comparing the area (AUC) under Receiver Operating Characteristics (ROC) curve [14]. After evaluating the ability of various color space components to differentiate the immunoreactive cell membrane from nonreactive components we found that B channel (inverted) from RBG and Y channel from CMYK representation are the most useful. The input intensity map used in further analysis is created as an element-wise product of these two components.

The alternative image map can be created based on local properties of the image. Analyzing many images we have noticed that local entropy of the image reflects very well the direction and distance of any pixel to the immunoreactive membrane. These areas of the membrane regions are characterized by a higher entropy than the other tissue regions. Based on this observation we have calculated the local entropy for each pixel of the image in the neighborhood size of 5×5 pixels. It was calculated for the product of B channel (inverted) of RBG representation and Y channel of CMYK. In medical practice the images are often blurred to same degree, so the blurred image map will be also investigated in our numerical experiments.

3.2 Types of Gradient

Based on the input map, the discrete gradient arrays have to be calculated in horizontal and vertical directions to implement effectively the snake active contour algorithm [16]. In this paper we study and compare four cases: 1) directional gradient, 2) gradient vector flow (GVF) [16], 3) directional gradient radially oriented to nuclei, and 4) GVF radially oriented to nuclei. The last two modifications of gradient are proposed by us and combined with an isotropic repulsion of the contour from the nuclei in direction to the immunoreactive cell membrane.

Horizontal and Vertical Directional Gradient. The directional gradient of the gray scale image I for any pixel is calculated in both directions (horizontal and vertical) and is defined as a difference between the intensity values of the neighboring pixels in both directions, respectively. If the horizontal and vertical positions of pixel are indexed by i and j, respectively, the directional gradient values are defined by

$$\begin{aligned} \rho_x(i,j) &= (I_{i,j+1} - I_{i,j-1})/2, \\ \rho_y(i,j) &= (I_{i+1,j} - I_{i-1,j})/2 \end{aligned} \tag{1}$$

They are compatible with the definition of the central finite difference. Their practical implementation is done using the dilation and erosion of the image by

a structuring element in the form of a horizontal or vertical line segment L. In this way

$$\rho_\alpha(i,j) = (\delta_{L_\alpha} - \epsilon_{L_\alpha})/2 \tag{2}$$

where the symbols δ and ϵ represent the dilation and erosion [12], respectively, and α denotes the horizontal or vertical direction. Although different spacing of the bordering pixels can be used in selection of the length L, the value one was applied in experiments.

Gradient Vector Flow. The modulus of the directional gradient in image processing is highly dependent on the distance of pixel to the immunoreactive cell membrane. However, the input image map has nonzero elements mainly in the regions of the immunoreaction, because the cytoplasms area is almost deprived of stain. This leads to the gradient map values close to zero. Additionally, some deformations of cells in the form of boundary concavities are also observed, especially when the initial location of the nucleus in the kidney cancer cells is far from the center. This fact reduces significantly the convergence of the active contour to the cell membrane, leading in some cases to the wrong results.

For this reason, the gradient vector flow (GVF) proposed by [16], was taken into account in our investigations. The main advantages of the GVF are its insensitivity to initialization and ability of process to move into the concave boundary regions. The GVF offers higher convergence of the snake model due to better orientation of the gradient vectors with respect to edges and also larger area of attraction. Denoting by $\rho_x(i,j)$ and $\rho_y(i,j)$ the directional gradients of edge map in the point (i,j) of the image, $u^n_{i,j}$ and $v^n_{i,j}$ the GVF components of this point in nth iteration, the iterative solution of GVF can be written in the form of difference equations [16]:

$$\begin{aligned} u^{n+1}_{i,j} &= u^n_{i,j} + \Delta t[\mu\nabla^2 u^n_{i,j} - (\rho_x^2(i,j) + \rho_y^2(i,j))(u^n_{i,j} - \rho_x(i,j))], \\ v^{n+1}_{i,j} &= v^n_{i,j} + \Delta t[\mu\nabla^2 v^n_{i,j} - (\rho_x^2(i,j) + \rho_y^2(i,j))(v^n_{i,j} - \rho_y(i,j))] \end{aligned} \tag{3}$$

In these expressions ∇^2 is the Laplacian operator and μ a regularization parameter. After some iterations this process leads to the proper values of GVF components.

Gradient Radially Oriented to Nuclei. The direction of the mentioned above gradient formulas is related to the local maxima of the snake model. Unfortunately, the experiments have shown, that in not all cases such direction is able to find the cell membrane. The cell nuclei in kidney cancer are frequently located in an acentric position. In this case gradient points to nearest edge, all points belonging to initial contour are attracted to that edge and this leads to the wrong results of localisation of the membrane segments(only one edge detected). To solve this problem we propose here the radially oriented gradient direction, which takes into account the pixel orientation toward cell nucleus. The horizontal $\rho_{R,X}$ and vertical $\rho_{R,Y}$ components of radially oriented gradient vector for the

pixel in the position (i, j) are described as follows

$$\begin{aligned} \rho_{R,X} &= \sqrt{\rho_X^2 + \rho_Y^2} \cdot cos[\phi_{i_0,j_0}(i,j)], \\ \rho_{R,Y} &= \sqrt{\rho_X^2 + \rho_Y^2} \cdot sin[\phi_{i_0,j_0}(i,j)], \end{aligned} \tag{4}$$

The symbol "$\cdot$" denotes the point-wise multiplication of two images, $\phi_{i_0,j_0}(i,j)$ the angle direction between the pixel position (i, j) and the central point (i_0, j_0) of the nucleus. In these expressions the orientation of the vector ρ toward the nucleus of the cell is important. The same modification of the gradient direction can be applied to the GVF.

After applying this approach to either classical directional gradient or GVF we achieve two important features of the algorithm: enhancement of the information of the gradient in the edge map and the direction of the gradient oriented radially to the nuclei.

Parametric Snake Model. Snakes, or active contours, are curves defined within an image that can move under the influence of internal forces within the curve itself and external forces derived from the image data [16]. The internal and external forces are defined so that the snake will conform the desired object boundary

The internal forces coming from within the curve itself control its tension and rigidity, whereas the external forces make it fit to objects. The snake curve represented in the form of vector $\mathbf{x}(s) = [x(s), y(s)]$ for the parameter $s \in [0, 1]$ is created by minimizing the energy functional in the spatial domain of an image

$$minE = \int_0^1 \tfrac{1}{2}[\alpha \left|\mathbf{x}'(s)\right|^2] + E_{ext}(\mathbf{x}(s))ds \tag{5}$$

where α and β are weighting parameters that control the snakes tension and rigidity, respectively. The first and second derivatives of snake are defined with respect to the parameter s. The external energy function E_{ext} (associated sometimes with the GVF) is taken from the input image map. In the latter case we use directly any representation of gradient map introduced above.

Particle Swarm Optimization. The proposed model of snakes requires selecting the set of seven parameters. They include a and from equation (5), the viscosity parameter, the weights of internal and external energy in the functional, and parameters corresponded with initial contours(circle) such as the radius and distance between the subsequent points that form the snakes curve [16]. Finding best solution in seven dimension space is complex task, thus optimization process is necessary. We have solved this optimization problem using the Particle Swarm Optimization (PSO) method.

PSO, originally attributed to Kennedy, Eberhart and Shi [5] and inspired by social behavior of bird flocking or fish schooling, is a computational method of optimization which applies the population (called a swarm) of candidate solutions (called particles). The particles keep track of their coordinates and also the coordinates of the entire swarm in the space. The movements of particles are

guided by their own best known position in the searchspace, taking into account the entire swarm's best known position. The particle swarm optimizer tracks the best value of the objective function, obtained so far by any particle in the neighborhood of it. When better positions are being discovered they will guide the movements of the entire swarm. The process is repeated and a satisfactory solution will eventually be discovered, although there is no guarantee of finding the global optimal solution.

PSO shares many similarities with evolutionary computation techniques. The system uses a population of random solutions and searches for optima by updating generations. However, unlike evolutionary algorithms, PSO has no evolution operators such as crossover and mutation. In PSO, the particles fly through the problem space by following the current optimum particles. The advantages of PSO over evolutionary algorithm are that PSO is easier to implement and there are only few parameters to adjust. Similarly to evolutionary algorithms PSO does not require that the optimization problem be differentiable, as is required by classic optimization methods such as gradient descent or quasi-Newton methods. PSO can therefore be applicable to optimization problems that are partially irregular, noisy, change over time, etc.

Final Membrane Localization System. The complete scheme of the final membrane localization system applied by us is presented in Fig. 2. It is composed of two main parts: 1) recognition of membrane using the snake and identification of membrane parts by applying segmentation of the high intensity immunoreactive areas and 2) localization of the nucleus in the cell. Both streams are cooperating together in assigning the recognized membrane to the particular cell and assessing the continuity of the membrane. This work is concerned mainly with the first task of application of snake to the membrane localization and association with the proper cell.

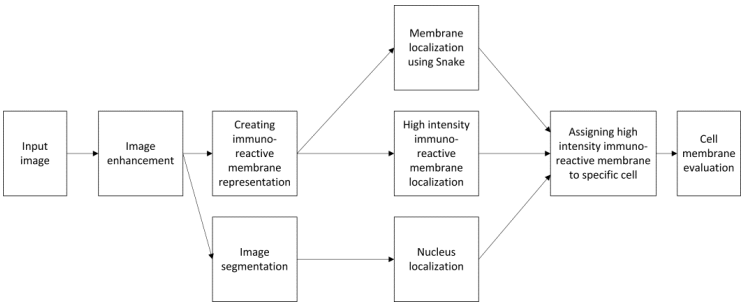

Fig. 2. The general scheme of image processing leading to the evaluation of the membrane parameters

4 Results

Aim of our work was to creating algorithm that estimates membrane continuity in the same way as an expert. To verify our approach the numerical experiments have been performed on two sets of data. The first one referred to the breast cancer and the second to the kidney cancer. Both cases required similar operations, described in the previous sections. The experiments have been performed using 100(testing set) cells representing the breast and kidney sets. The results will be presented in the numerical and graphical forms. We compare the statistical results of our automatic system (AS) to the results of an expert. The main points of comparison are the estimation of continuity of the identified membrane by AS and by an expert and also the Hausdorff distance. The Hausdorff distance represents the longest of all the distances from a point in one set to the closest point in the other set.

Table 1. The numerical results of membrane continuity estimation in breast cancer made by an expert and the automatic system

Algorithm	Hausdorf distance	Membrane continuity Expert	Membrane continuity AS	Absolute difference	Standard deviation	Accuracy of assigning membrane to a cell
CM pl CDG CG	20.90	0.71	0.59	0.14	0.11	100%
CM pl CDG RO	20.63	0.71	0.59	0.13	0.11	100%
CM pl GVF CG	22.64	0.71	0.72	0.09	0.11	97%
CM pl GVF RO	17.95	0.71	0.70	0.08	0.09	98%
CM bl CDG CG	22.26	0.71	0.61	0.13	0.12	100%
CM bl CDG RO	21.85	0.71	0.59	0.14	0.11	100%
CM bl GVF CG	22.00	0.71	0.73	0.10	0.10	98%
CM bl GVF RO	19.85	0.71	0.74	0.11	0.16	92%
EN pl CDG CG	23.81	0.71	0.43	0.28	0.15	100%
EN pl CDG RO	24.60	0.71	0.44	0.27	0.14	100%
EN pl GVF CG	22.56	0.71	0.68	0.09	0.08	100%
EN pl GVF RO	18.14	0.71	0.71	0.08	0.08	98%
EN bl CDG CG	23.21	0.71	0.52	0.20	0.14	100%
EN bl CDG RO	22.93	0.71	0.55	0.17	0.14	100%
EN bl GVF CG	19.10	0.71	0.74	0.09	0.10	96%
EN bl GVF RO	18.48	0.71	0.73	0.09	0.12	98%
Direct watershed	17.31	0.71	0.73	0.10	0.07	64%

Table 1 depicts the numerical results of experiments concerning breast cancer. They are given in the form of mean values of Hausdorff distance measure (in pixels) and membrane continuity, estimated for the set of 100 breast cancer cells at application of different versions of the algorithms. The Hausdorff distance depicts the highest distance between the membrane discovered by snake and membrane

segments recognized by application of the hourglass shape structuring element combined with watershed algorithm, presented in [15]. The continuity is defined as the ratio of the summed lengths of discovered membrane segments to the total length of membrane estimated by the snake model. The next two columns of the table represent the means per cell and standard deviations regarding the absolute differences between the estimations of the membrane continuity made by AS and by an expert. The last column depicts the statistical accuracy of assigning the membrane to the proper corresponding cell. The first 8 rows present the results of direct application of color map (CM) and the last 8 the entropy (EN) approach. The last row of the table represents the direct application of watershed algorithm. We compare the efficiency of different forms of gradient generation (classical directional gradient - CDG and GVF). The radially oriented gradient estimation is denoted in the table by (RO) and the classical form of directional gradient is denoted by (CG). The results refer to the plain images (pl) and to the blurred ones (bl). The best accuracy has been obtained for an entropy map at application of radially oriented GVF gradient estimation. In this case we got full agreement of the mean value of the membrane continuity estimated by our automatic system and by an expert, at very small value of standard deviation. Direct watershed algorithm was only slightly worse than snake but only 64% were assigned.

Table 2. The numerical results of membrane continuity estimation in kidney cancer made by an expert and the automatic system

Algorithm	Hausdorf distance	Membrane continuity Expert	Membrane continuity AS	Absolute difference	Standard deviation	Accuracy of assigning membrane to a cell
CM pl CDG CG	19.34	0.70	0.56	0.16	0.13	100%
CM pl CDG RO	19.10	0.70	0.58	0.15	0.10	100%
CM pl GVF CG	22.63	0.70	0.62	0.13	0.10	99%
CM pl GVF RO	31.68	0.70	0.56	0.17	0.12	72%
CM bl CDG CG	19.56	0.70	0.53	0.19	0.13	100%
CM bl CDG RO	16.63	0.70	0.61	0.12	0.09	100%
CM bl GVF CG	19.91	0.70	0.65	0.11	0.09	99%
CM bl GVF RO	19.88	0.70	0.67	0.08	0.07	98%
EN pl CDG CG	16.90	0.70	0.52	0.19	0.12	100%
EN pl CDG RO	17.09	0.70	0.52	0.20	0.12	100%
EN pl GVF CG	16.20	0.70	0.48	0.23	0.12	100%
EN pl GVF RO	16.59	0.70	0.47	0.24	0.12	100%
EN bl CDG CG	19.99	0.70	0.46	0.25	0.13	100%
EN bl CDG RO	16.27	0.70	0.50	0.21	0.11	100%
EN bl GVF CG	18.77	0.70	0.60	0.13	0.11	100%
EN bl GVF RO	17.11	0.70	0.62	0.12	0.12	81%
Direct watershed	18.36	0.70	0.59	0.14	0.13	99%

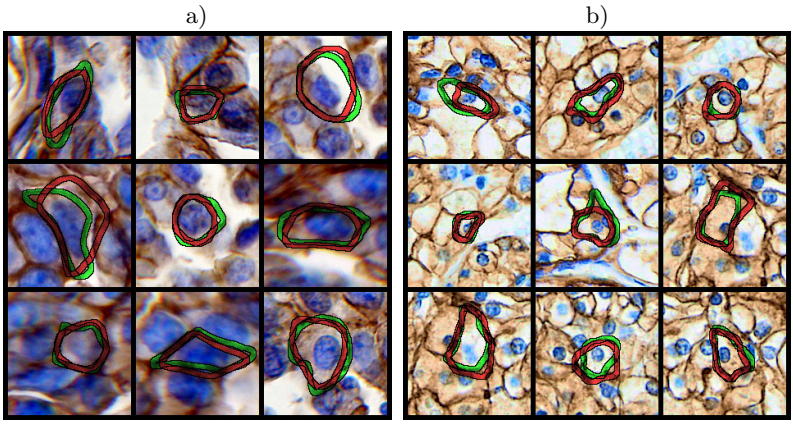

Fig. 3. The illustrative results of membrane localization in the cell images of breast cancer (a) and kidney cancer (b). The images correspond to these in Fig.1.

Table 2 presents the results concerning kidney cancer at different variants of the snake algorithm and image representation. The highest agreement of the membrane continuity (0.67 of AS against 0.70 in expert estimation) has been achieved in colour map representation of the image and radially oriented GVF gradient estimation. This time the direct application of watershed was highly inefficient (membrane continuity estimation 0.59 against the value 0.70 of an expert).

The results of image analysis are also presented in the graphical form. Fig. 3 depicts the results of membrane localizations for 9 chosen cells. They have been made by using the best snake algorithm (denoted by red color) and the expert estimation (green color) and refer to the original images of cells illustrated in Fig. 1. High similarity of the results of membrane localizations obtained by our system and expert is visible in the most cases.

5 Conclusion

The paper has presented the modified snake approach to the automatic recognition of the HER2/neu cell membrane and its association with the neighbouring cell. The main effort has been directed toward assigning the snake model of the membrane with the proper cell of the image. The work has been concentrated on comparing different methods of gradient generation and application of swarm optimization in solving the snake model in the breast and kidney cancer samples. The recognized membrane shape has enabled proposing an automatic method of the membrane continuity estimation, an important factor in the pathomorphological evaluation of breast and kidney cancers.

The experimental results have shown high efficiency of this approach to the image segmentation in the membrane localization task. The best radially oriented GVF method applied in snake model was able to generate statistical results

concerning the continuity of membrane with excellent mean value agreement to the expert results and of the smallest standard deviation.

It should be noted, that our computerized system is fully automatic. Hence the recognition of the nuclei and membrane associated with the cell is done according to an automatic procedure defined within the algorithm. On the other hand the human expert selects the nuclei and membrane according to his professional knowledge, blind to the selection results of an automatic system. This is the reason of slight differences between the recognized membrane shapes observed in the segmentation results.

Acknowledgments. This work has been supported by the National Centre for Research and Development (PBS2/A9/21/2013 grant), Poland.

References

1. PATHWAY HER-2/neu (4B5) – user manual. Ventana Medical Systems, Tucson (2009)
2. Matlab Image Processing Toolbox: users guide. MathWorks, Natick (2012)
3. Grala, B., Markiewicz, T., Kozlowski, W., Osowski, S., Slodkowska, J., Papierz, W.: New automated image analysis method for the assessment of ki-67 labeling index in meningiomas. Folia Histo. Cyto. **47**(4), 587–592 (2009)
4. Kasson, P., Huppa, J., Davis, M., Brunger, A.: A hybrid machine-learning ap-proach for segmentation of protein localization data. Bioinformatics **2**(19), 3778–3786 (2005)
5. Kennedy, J., Eberhart, R.: Swarm Intelligence. Morgan Kaufmann, San Francisco (2001)
6. Latif, Z., Watters, A., Bartlet, J., Underwood, M., Aichison, M.: Gene amplification and overexpression of her2 in renal cell carcinoma. BJU Intern. **89**, 5–9 (2002)
7. Les, T., Markiewicz, T., Osowski, S., Cichowicz, M., Kozlowski, W.: Automatic evaluation system of FISH images in breast cancer. In: Elmoataz, A., Lezoray, O., Nouboud, F., Mammass, D. (eds.) ICISP 2014. LNCS, vol. 8509, pp. 332–339. Springer, Heidelberg (2014)
8. Lezoray, O., Elmoataz, A., Cardot, H., Gougeon, G., Lecluse, M., Elie, H., Revenu, M.: Segmentation of colour images from serous cytology for automated cell classification. Anal. Quant. Cytol. Histol. **22**, 311–322 (2000)
9. Littlejohns, P.: Trastuzumab for early breast cancer: evolution or revolution? Lancet Oncology **7**(1), 22–33 (2006)
10. Logan, J., Edwards, K., Saunders, N.: Real-Time PCR: Current Technology and Applications. Caister Academic Press, Norfolk (2009)
11. Naegel, B., Passat, N., Ronse, C.: Grey-level hit-or-miss transforms part i:unified theory. Pattern Recogn. **40**, 635–647 (2007)
12. Soille, P.: Morphological Image Analysis, Principles and Applications, 2nd edn. Springer, Berlin (2003)
13. Tabakov, M., Kozak, P.: Segmentation of histopathology her2/neu images with fuzzy decision tree and takagi-sugeno reasoning. Comput. Biol. Med. **49**, 19–29 (2014)

14. Tan, P., Steinbach, M., Kumar, V.: Introduction to data mining. Pearson Education Inc., Boston (2006)
15. Wdowiak, M., Markiewicz, T., Osowski, S., Swiderska, Z., Patera, J., Kozlowski, W.: Hourglass shapes in rank grey-level hit-or-miss transform for membrane segmentation in HER2/neu images. In: Benediktsson, J.A., Chanussot, J., Najman, L., Talbot, H. (eds.) Mathematical Morphology and Its Applications to Signal and Image Processing. LNCS, vol. 9082, pp. 3–14. Springer, Heidelberg (2015)
16. Xu, C., Prince, J.: Snakes, shapes, and gradient vector flow. IEEE Trans. Image Processing **7**(3), 359–369 (1998)